JOURNAL OF MATERIALS SCIENCE 13 (1978) 1471–1479

Wear damage of MgO single crystals

TADAAKI SUGITA
Department of Precision Engineering, Kanazawa University, Kanazawa, Japan
TAKANORI HASEGAWA
Hydraulic Engineering Division, Fujikoshi Ltd., Toyama, Japan

Mechanisms of surface and sub-surface wear damage in MgO single crystals were investigated by scratching with two sintered alumina sliders, having tip radii of 60 and 120 μm, using a simple scratching apparatus in a controlled atmosphere. The degree of surface and sub-surface cracking is dependent on the shape of the slider and the normal contact load, which are related to the penetration into the crystal. The chevron crack on the (001) plane in the [100] sliding direction consists of cracks intersecting at an angle of 90°, and with a spread angle of about 120°, and the normal crack. The nature of the sub-surface damage is investigated; a parallel crack develops in front of the slider and an oblique crack propagates towards the front of the slider. Then an internal normal crack is formed between the oblique crack and the parallel crack. In the [110] direction, the oblique crack initiates from the top of the normal crack under the surface, and the parallel crack continues from the oblique crack. This wear damage is explained by the dislocation interactions occurring due to the distribution of resolved shear stresses during sliding. The wear caused by the chevron crack is a factor of 10 higher than that with plastic flow. Internal cracks do not have a direct influence on the increase of wear.

1. Introduction

Wear of brittle materials, especially some ionic materials, is dominated by brittle fracture, although the evaluation of the relationship between fracture and wear is very complicated. MgO in single crystal form is a convenient material to study the wear mechanism because it has the simple NaCl crystal structure and its fracture is closely related to its crystallographic characteristics. In this crystal, it is supposed that surface damage and wear in sliding are strongly dependent upon the anisotropy of the bulk material [1, 2].

Keh *et al.* [3] and Kear *et al.* [4] discussed some dislocation interactions in simple crystals. Stucke and Wronski [5] observed various complex dislocation arrays on pressurized surfaces of MgO single crystals, and also found that the {1 1 0} and {1 0 0} cracks were formed at a relatively high pressure, 1.0 GN m^{-2}. Stokes and others [6–8] reported that the dislocation interaction under compressive and bending stresses caused pile-ups of dislocations by slip which initiated microcracks. Pask and Langdon [9] indicated that the cleavage fracture of MgO under tensile stress was developed by microcracks formed by dislocation reactions on two {1 1 0} slip planes, as predicted in the Cottrell model [10]. These investigations are very useful in discussing the fracture mechanism of MgO single crystals during sliding.

According to Steijn [11], the observed typical surface cracks on the {1 0 0} rubbing plane when NaCl, LiF and MgO, having the sodium chloride crystal stucture, were scratched in the ⟨1 0 0⟩ direction were explained on the basis of dislocation interactions on the {1 1 0}⟨1 1 0⟩ slip systems. The dislocation interactions are caused by the double dislocation pile-up on two {1 1 0} slip planes intersecting at 120° as discussed by Keh *et al.* [3]. Also, he had an opinion that wear in ionic crystals is fundamentally a process of microfracture [12]. Bowden and Hanwell [13] and Bowden and Brookes [1] showed the wear damage and discussed the mechanism of wear damage caused by dislocation interactions, like chevron cracking and

sub-surface cracking, in MgO single crystals from the viewpoint of the crystallographic slip systems and based on the resolved shear stress [1]. A similar result was also obtained from deformation in the region of indentation in hardness measurements of MgO single crystals [2].

Buckley [14] predicted that the wear mechanism in some materials might be associated with fatigue failure of the surface material between the surface and the sub-surface crack realized after repeated loading. His prediction is interesting and provides a likely explanation for wear accompanied by surface fragmentation.

The present paper described the wear damage and the crystallographic fracture patterns observed on the surface and in the sub-surface of MgO single crystals during sliding, in particular the sub-surface damage prior to surface wear. This damage may be discussed with reference to the dislocation interaction. The results should be able to provide a basic wear mechanism for some ionic materials.

2. Experimental procedure

Sliding tests were performed using the machine shown in Fig. 1. The specimen of MgO single crystal with a specified crystallographic plane was mounted on the moving stage, which was pulled or pushed by the driving shaft of the motor at a speed of 0.5 mm sec^{-1}, and was rubbed by a static conical indenter (slider) made of sintered alumina. Frictional behaviour was observed on a Braun tube oscilloscope. The surface and sub-surface damage near the slider was observed through an optical microscope during sliding, while the crack formation and propagation were caught by a high speed movie camera. The relative humidity in the regulated experimental environment was kept constant at 20%.

MgO single crystals* with low dislocation densities were used for these experiments. The (100) plane specimen was obtained from an ingot by cleaving, while the {110} plane specimen was formed by grinding with a diamond grinding wheel of #400 grit. These specimens were etched in orthophosphoric acid at 150° C for 5 min in order to remove the surface damage and the work-hardened layer produced in sizing the specimens. Sintered alumina sliders with tip radii of 60 and 120 μm were prepared by grinding hot-pressed pieces to circular cones with an apical angle of 100°, and mirror polishing them with diamond paste.

The depth and width of wear tracks were determined from the profile diagrams by a profilometer.

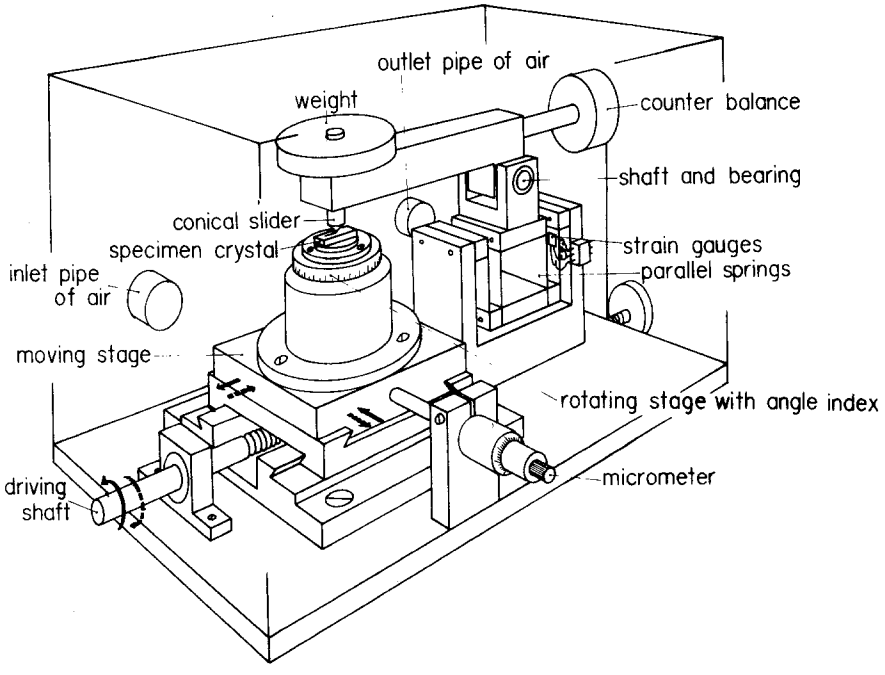

Figure 1 Schematic diagram of friction apparatus.

* Tateho Chemical Industry Co. Inc. (Japan).

Since the MgO specimen were quite transparent, the observation of damage was not only possible on the surface, but also in the sub-surface; the details were obtained by scanning electron microscopy. For the observation of dislocation etch pits, the etchant used consisted of NH_4Cl, 10%; HCl, 30%; and water, 60%.

3. Results

3.1. Surface damage on the {100} plane

Fig. 2 shows the typical modes of the chevron crack and a fracture pattern in the chevron wing with [100] sliding direction on the (001) plane of MgO single crystals. In (a), two types of crack, which are the cracks with an intersecting angle of 90° and with a spread angle of about 120°, are observed as the chevron crack. Large chevron cracks are produced under considerable alternation of friction. However, it is possible that small chevron cracks are formed even under low friction if the normal cracks along the sliding direction are formed, as shown in (b). The inside of the chevron wing with an angle of 120° is revealed in (c). The chevron wing consists of the oblique wall, the normal wall and the cleavage steps. After the chevron with an intersecting angle of 90° is initiated near the wear track, the wing may extend towards the outside of the wear track, forming an intersecting angle of 120°. These chevron cracks do not appear when the normal load is decreased; then the cracks develop only along the {110} slip planes [1, 11]. In the [100] sliding direction, ploughing of the wear track should be noticed in Fig. 2 as typical of plastic deformation. No pile-up was observed in the [110] direction, contrary to the results of the profile test by Bowden and Brookes [1].

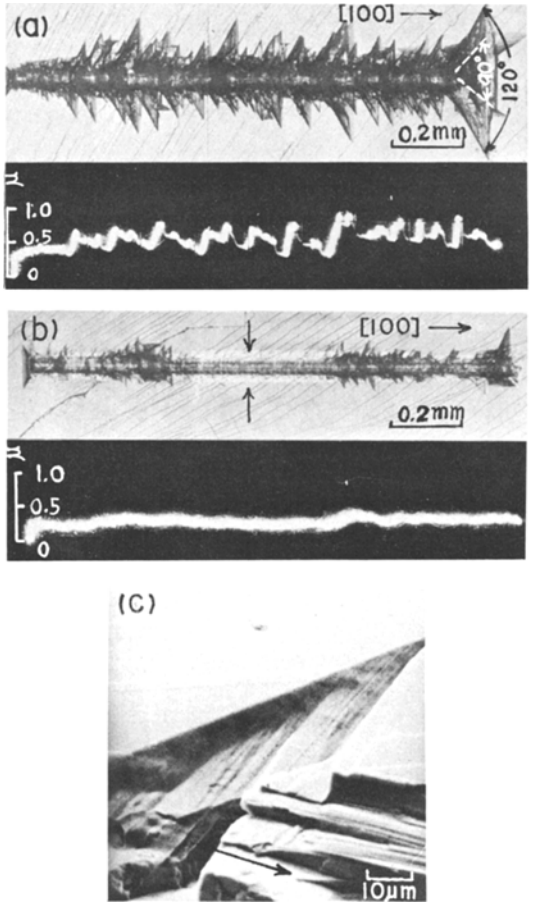

Figure 2 Surface damage on (0 0 1) plane as affected by normal contact load and tip radius of slider and frictional behaviour. (a) The large chevron crack configuration, (b) the small chevron crack and the ploughing (indicated by black arrows) and (c) the inside of the chevron wing in (a). Selected normal load and tip radius of slider are 400 g and 60 μm in (a), and 400 g and 120 μm in (b). [1 0 0] in each photograph is the sliding direction.

The relationship between the normal load and the depth of wear track, which is approximately equal to the penetration depth of the slider, is shown in Fig. 3. The chevron crack is observed when the penetration of the slider is deepened above the depth of wear of 0.5 μm; the critical loads for chevron crack formation correspond to 100 g for the sharp slider (60 μm) and to 350 g for the blunt slider (120 μm). Sliding with the slider penetrating deeply removes much of the surface

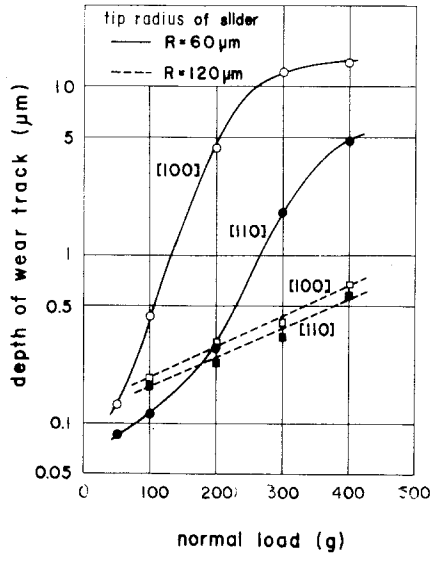

Figure 3 Changes in depth of the wear track as the functions of normal load, sliding direction and tip radius of slider. The sliding plane is the (0 0 1) plane.

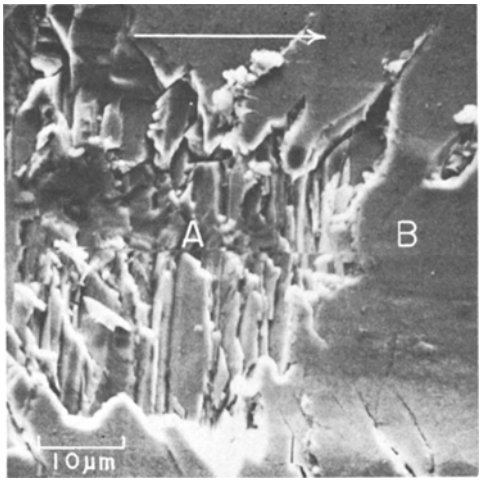

Figure 4 Brittle fracture by a sharp slider observed on a pre-formed smooth wear surface. Surfaces A and B were rubbed by a slider with tip radius of 60 μm under a normal load of 100 g, and by a slider with tip radus of 120 μm under a normal load of 400 g, respectively. Sliding surfaces and directions are (0 0 1) and [1 0 0], respectively.

material, including that loosened by brittle fracture. This result suggests that the actual wear of MgO may be affected by the shape of the asperities on the surface of the harder material at the point of contact.

On the other hand, the two typical coefficients of friction, which are $\mu = 1.0$ in brittle fracture accompanied by large chevron cracks and $\mu = 0.2$ in plastic flow (see Fig. 2), are taken as the normal frictional behaviour [1]. Since the penetration and friction of a slider with a smooth blunt tip are very low, and constant over a number of slidings without any surface cracks, the wear rate is expected to be much lower. In this case, the continuous formation of a thin film by plastic flow occurs on the wear surface, resulting in a wear mechanism that is considerably different from that producing chevron cracks. Fig. 4 shows a brittle wear surface which was scratched by the sharp slider after the surface was smoothed by the blunt slider. If the 10 slidings by the sharp slider are repeated on the surface in Fig. 4, the depth of wear reaches locally to the internal parallel crack formed below the surface, as shown in Fig. 5. This wear behaviour is a typical example of surface fracture. Thus, the wear of MgO is significantly influenced by the mode of wear damage.

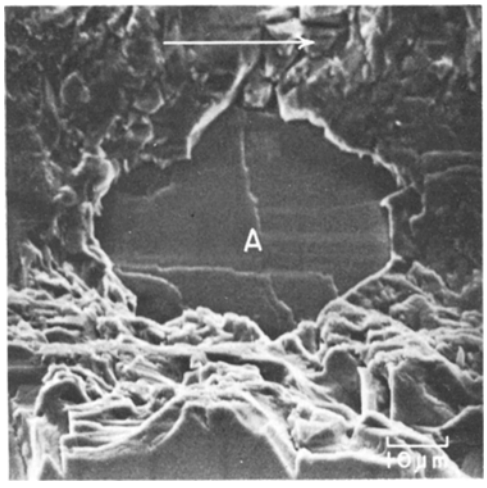

Figure 5 Surface of internal parallel crack, A, observed in the wear track after ten repeated slidings similar to the conditions for the sharp slider in Fig. 4.

3.2. Sub-surface damage on the {100} plane

The non-destructive observation of internal cracks formed underneath the surface of MgO single crystals is possible through the bulk because of the transparency of the MgO. Fig. 6 is an example of such continuous observation. Photographs of the formation and propagation of internal cracks generated under the surface, during sliding in the ⟨1 0 0⟩ direction, were taken with a high speed movie camera. The internal parallel crack always develops parallel to the sliding surface and in front of the centre of the slider. The oblique crack, which intersects at 45° to the surface and initiates from the bottom of the chevron crack, propagates towards the front of the slider, but the crack propagation is stopped when the slider passes over the crack. Subsequently the normal crack, which is perpendicular to the surface, is formed between the top of the oblique crack and the parallel crack. This normal crack never penetrates beyond the parallel crack. Shadow A at 0.01 sec resulted from bulk deformation in front of the slider, and vanishes with the movement of the slider at 0.13 sec.

The crystallographic orientations for three typical internal cracks are given on the cross-section of the wear surface, as shown in Fig. 7. The parallel crack is cleavage fracture of the {1 0 0} plane and the oblique crack may be related to strongly accelerated slip on the {1 1 0} planes. Also, tension produced behind the slider may be enough to extend the normal crack. Such a configuration of internal cracks can be influenced by the normal load and tip radius of the slider. A small radius is equivalent to a heavy load. Under a light load, only the parallel crack remains without any surface

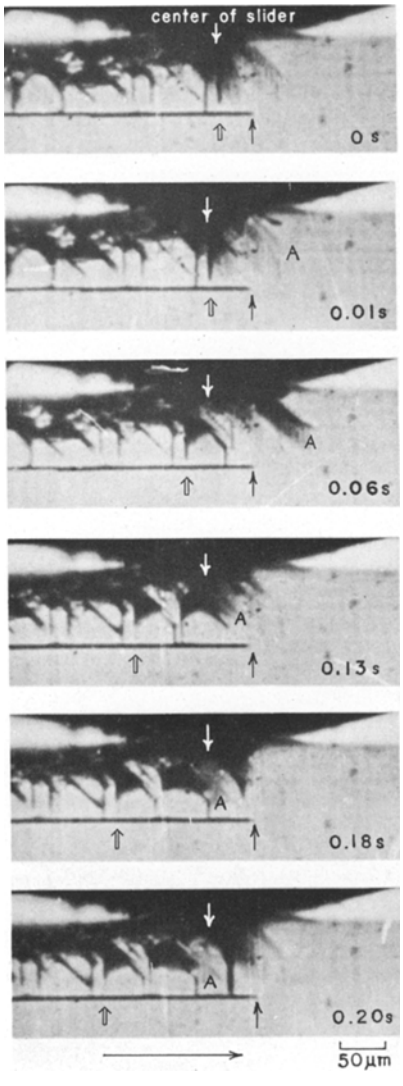

Figure 6 Initiation and propagation of internal cracks during sliding. The number in each photograph is the lapsed time from zero seconds. Photographs are taken with a high speed movie camera. The double black arrow is a reference point for observation. The single black arrow is the top of the internal parallel crack, and the white arrow is the centre of slider, at each lapse time. The sliding surface was the (0 0 1) plane; sliding direction, [1 0 0] direction; radius of slider, 120 μm; normal load, 600g.

damage. The width and distance from surface of the parallel crack and the width of the wear track are shown in Fig. 8 as a function of normal load.

The width of the parallel crack, which would be associated with the width of a microcrack formed from dislocation interaction of two intersecting {1 1 0} slip planes, is always a factor of two wider than that of the wear track. It appears that the dislocation interaction at the place of maximum shear stress enhancement under the surface is associated with the distance from the surface of the parallel crack. The probable dislocation interaction required for the formation of a parallel crack will be discussed in the following section.

On the other hand, the internal cracks are not clear, as shown in Fig. 9, when the sliding direction is in the ⟨1 1 0⟩ direction, because the crack surface on the (1 0 1) slip plane is inclined to the side from which it is observed. The configuration of cracks is illustrated in Fig. 9. The surface cracks caused by dislocation interaction develop in three directions, which are in front of the slider and both sides of the wear track [1]. The fracture of {1 1 0} slip planes inclined at 45° to the sliding direction appears as oblique cracks on the (1 0 1) and (0 1 1) planes, and the enveloped area, which consists of surface cracks leading from two oblique cracks and two surface cracks developed perpendicular to sliding direction, corresponds to the chevron crack. The parallel crack, in this case, develops from the top of each oblique crack, but

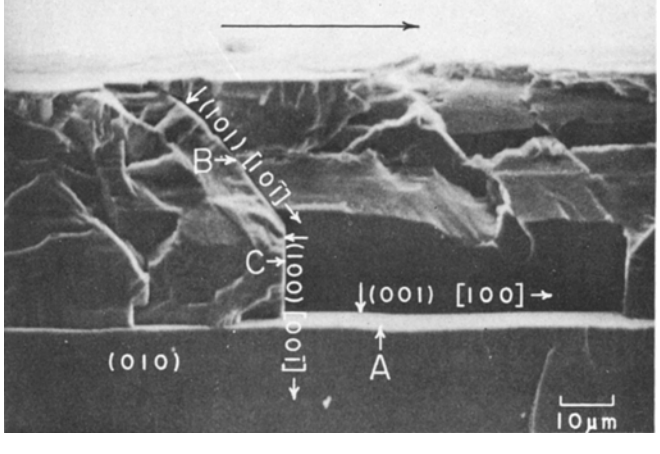

Figure 7 Cross-section of internal cracks formed under the wear surface. A is the parallel crack, B the oblique crack and C the normal crack. Normal load, 600 g; tip radius of slider, 120 μm.

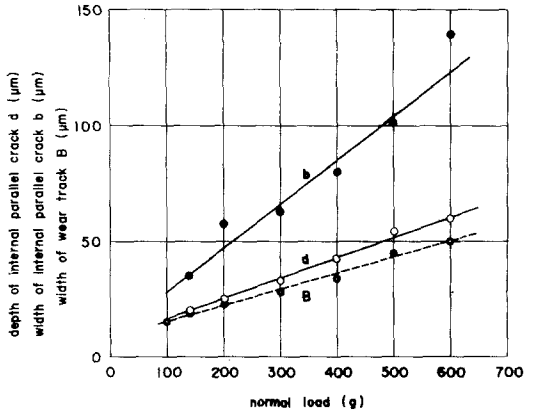

Figure 8 Changes of depth and width of internal crack and width of wear track as influenced by the normal load during sliding in the [1 0 0] direction on the (0 0 1) plane. Radius of slider is 120 μm.

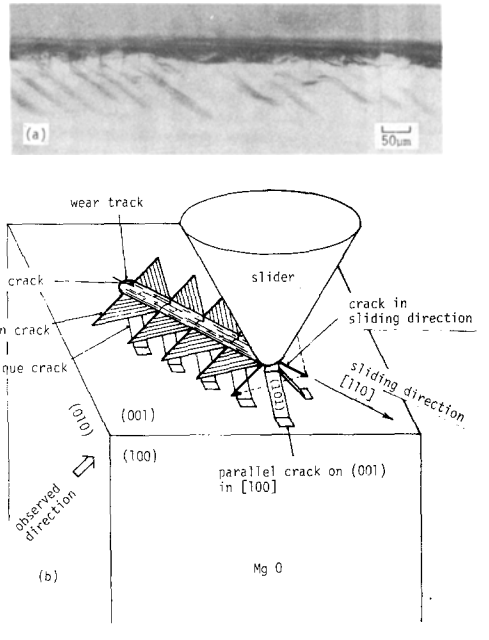

Figure 9 Internal crack configuration in sliding in the [1 1 0] direction on the (0 0 1) plane. (a) As observed from the side of the inclined (1 0 1) plane as shown in (b). Radius of slider and normal load are 120 μm and 700 g, respectively.

the extended length is limited within the distance to the next oblique crack.

It is important in understanding the wear mechanism to know how the internal cracks change after repeated sliding. Fig. 10 shows the change of internal cracks in relation to the number of slidings.

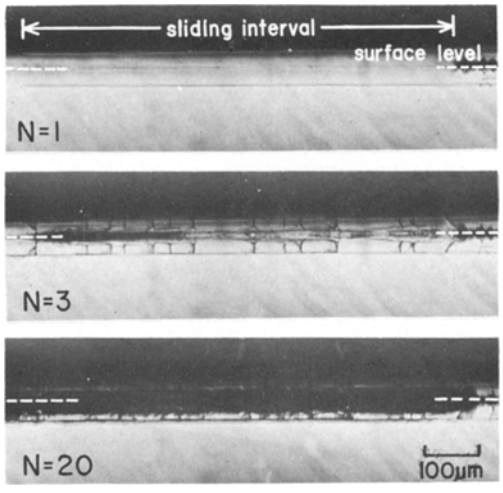

Figure 10 Changes in internal cracks by repeated sliding. N in each photograph is the number of slidings. Sliding surface was (0 0 1) plane; sliding direction, [$\bar{1}$ 0 0]; radius of slider, 120 μm; normal load, 300 g. Surface level is indicated in each photograph.

The internal crack is only parallel cracks without any other kind of crack, when $N = 1$. With $N = 3$, many normal cracks initiate along the cleavage planes and are stopped at the parallel crack. Although the material between the surface and the parallel crack is markedly deformed with increasing sliding frequency, the wear surface was not torn off from the parallel crack even when $N = 20$, contrary to Buckley's prediction [14]. However, it is possible that the thin surface layer of the wear track in plastic flow is gradually torn off with repeated sliding [15, 16]. On the other hand, the material subjected to wear with severe surface damage, like chevron cracks, is removed locally from the parallel crack, as shown in Fig. 5. The wear volume caused by brittle fracture is a factor of 10 higher than that with plastic flow. These results indicate that the wear depends remarkably on brittle fracture. Nevertheless, the internal cracks are basically independent of the progressing wear.

4. Discussion

4.1. Formation of chevron cracks

Fig. 11 shows the resolved shear stress distributions in relation to sliding direction and the coefficient of friction on the (001) plane of MgO single crystals [1, 11]. In this figure, the {1 1 0}45°a indicates two slip planes which exist on either side of the slider, and the {1 1 0}45°b means two slip planes which are arranged in front and behind the

slider. The $\{1\,1\,0\}90°$ shows two slip planes which intersect at 90° to the (001) plane and intersect at 45° in the ⟨100⟩ direction [1, 17].

When sliding occurs on the (001) plane with low friction in the [100] direction, the surface cracks which are formed on either side of the wear track intersect each other at 90°. Then, the following dislocation interactions [11] make the cracks $1/2\ [10\bar{1}] + 1/2\ [0\bar{1}1] = 1/2\ [1\bar{1}0]$ and $1/2\ [101] + 1/2\ [011] = 1/2\ [110]$. These interactions support the observations that the resolved shear stresses with low friction are enhanced on the $\{1\,1\,0\}45°$a slip planes slipping in the $[0\,\bar{1}\,1]$ and [011] slip directions, and on the $\{1\,1\,0\}45°$b slip plane gliding in the $[10\bar{1}]$ slip direction. Additional evidence is the arrays of dislocation etch pits on either side of the wear track [1]. In contrast to the low friction, the coefficient of friction varies with time between about 1.0 and 0.2 when the large chevron cracks are formed (see Fig. 2). Bowden and Brookes [1] reported that the large chevron cracks are formed with a coefficient of friction of 0.9, and it may be necessary to know the process of crack formation. We observed the process of crack formation with a high speed movie camera. A crack intersecting at 90° was formed under the low friction in front of the slider. The normal crack then caused by cleavage of the (100) plane and the crack with a spread angle of about 120° were then likely to develop behind the slider at the time under high friction. The possibility of dislocation reaction may not be considered under high friction because the resolved shear stress in the high coefficient of friction does not act on the $\{1\,1\,0\}45°$b slip plane, as indicated in Fig. 11. Dislocations on the $\{1\,1\,0\}45°$a and $\{1\,1\,0\}$ $45°$b slip planes pile up during the low friction period and interact with each other to make the surface cracks. Subsequently, the tensile force produced behind the slider easily cleaves the surface normal to the wear track, because the normal stress in the period of high friction compresses the material in front of slider.

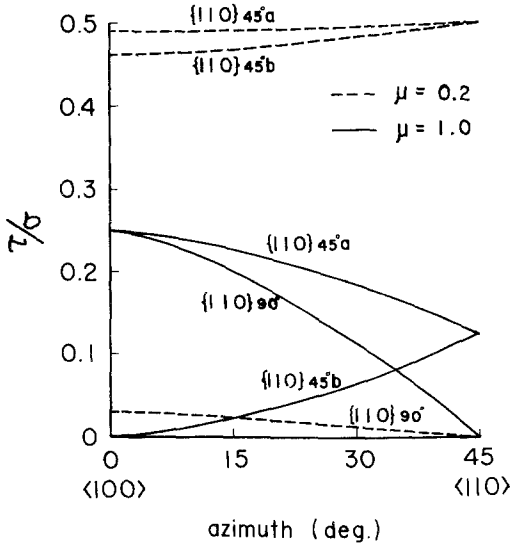

Figure 11 Influence of azimuth on distribution of resolved shear stress for sliding with coefficients of friction of 0.2 and 1.0.

Concurrently, the wing of the chevron crack with spread angle of about 120° develops, and joins to the edge of the normal crack when the coefficient of friction rises to a higher value in the case of the large chevron cracks. A number of the cleavage steps in the chevron wing are caused by the connection of the normal crack and the chevron crack (see Fig. 2). It is possible that the dislocation interaction of the tension behind the slider causes the formation of the extended chevron wing. The resolved shear stress distributions in a region affected by the normal crack and the internal parallel crack may be considerably changed from that in Fig. 11. If the resolved shear stresses under high friction are generated on the $\{1\,1\,0\}$ $45°$b slip plane, and are decreased on the $\{1\,1\,0\}$ $45°$a slip plane in the [100] sliding direction, two dislocation reactions, which are $1/2\ [1\,1\,0] + 1/2\ [101] = 1/2\ [2\,1\,1]$ and $1/2\ [1\bar{1}0] + 1/2\ [101] = 1/2\ [2\,\bar{1}\,1]$, are likely to occur. These reactions suggest the formation of a chevron wing with a spread angle of about 120°. According to Kear *et al.* [4], since these reactions involve an increase in the elastic energy, the two dislocations related to the reaction may try to repel one another along the intersection line. However, in this experiment the stress concentration at the top of the normal crack may cause these dislocation interactions to occur. Also, the high coefficient of friction is not necessary to form the chevron wing because the chevron crack is produced even with shallow penetration of the slider (or low coefficient of friction) if the tension behind the slider is enough to cleave the (100) plane, as shown in Fig. 2.

The three cracks formed near the wear track during sliding in the [110] direction are expected from the following three dislocation interactions

of the $\{1\,1\,0\}45°$a and $\{1\,1\,0\}45°$b slip planes. The equations for the crack normal to the sliding direction are $1/2\ [0\,1\,\bar{1}] + 1/2\ [\bar{1}\,0\,1] = 1/2\ [\bar{1}\,1\,0]$ and $1/2\ [1\,0\,\bar{1}] + 1/2\ [0\,\bar{1}\,1] = 1/2\ [1\,\bar{1}\,0]$. The crack observed at the top of the slider and parallel to the sliding direciton (see Fig. 9) is the result of the equation $1/2\langle 1\,0\,\bar{1}\rangle + 1/2\ \langle 0\,1\,1\rangle = 1/2\ \langle 1\,1\,0\rangle$. If sliding is continued uniformly after completion of the crack formation derived from the above dislocation interactions, the $\{1\,1\,0\}45°$a and $\{1\,1\,0\}45°$b slip planes in the surface layer surrounded by these three cracks are discontinuously and intermittently fractured with slip, because of the division of the components of the tensile force into the [100] and [010] directions. Consequently, when sliding is in the [110] direction, the chevron cracks converge in this direction.

4.2. Formation of internal cracks

Parallel cracking occurs more easily than oblique and normal cracking; cracks are observed even under the low friction condition without any surface cracks. It is noticed that the parallel crack formation in front of the slider is closely related to the site of the maximum shear stress. The crack is formed in the sub-surface in front of the slider (see Fig. 6), where it occurs at a distance of half the width of the wear track from the centre of the slider and at a depth from the surface equal to the width of the wear track (Fig. 8), while the location of the maximum shear stress in front of the slider is approximately at the position of the parallel crack observed in this experiment. The shear stress is calculated from two-dimensional elastic contact stress analysis [18] under sliding contact stress with a coefficient of friction of 0.2. It is, however, found that there is a small difference between the experimental depth of the parallel crack and the theoretical depth. The actual depth of the maximum shear stress from the surface should be greater than that for the theoretical calculation because of the effect of plastic deformation. From these considerations it is assumed that dislocation interactions caused by the intersections of two $\{1\,1\,0\}45°$a slip planes below the slider participate in the formation of parallel cracks. The dislocation reactions, $1/2\ [0\,\bar{1}\,\bar{1}] + 1/2\ [0\bar{1}1] = [0\,\bar{1}\,0]$ and $1/2\ [0\,1\,\bar{1}] + 1/2\ [0\,1\,1] = [0\,1\,0]$, may form the crack nuclei in conformity with the Cottrell model [10], and this crack is capable of cleaving the (001) plane. The width of the crack in Fig. 8 will be determined by the interacted width of the dislocations.

If normal stress through the slider is increased, the $\{1\,1\,0\}45°$b slip plane in front of the slider may be fractured by the increased shear stress, in accordance with the prediction by Stokes *et al.* [7], and the oblique crack will thus be able to propagate under this stress condition. The crack is initiated from the position of the centre of the slider and propagates toward the sliding direction, as observed in Fig. 6. The starting point of the crack is usually at the bottom of the chevron crack. The shear stress which is causing the oblique crack on the $\{1\,1\,0\}45°$b slip plane decreases as the slider moves over the crack, and crack propagation ceases when the centre of the slider on the surface overtakes the position of the crack. Subsequently, the (100) plane of the top of the oblique crack is cleaved by the tensile stress generated behind the slider as soon as the slider goes over the oblique crack. This cleavage crack is the internal normal crack.

5. Conclusions

From the experimental results obtained on the wear damage of MgO single crystals in preferential crystallographic orientation during sliding, the following conclusions are drawn;

(1) On the $\{1\,0\,0\}$ plane, the crack formation is caused by the dislocation interactions of the $\{1\,1\,0\}\langle 1\,1\,0\rangle$ slip systems, which are derived from the distribution of resolved shear stresses during sliding, and the cleavage crack on the $\{1\,0\,0\}$ plane. The coefficient of friction in the formation of the chevron crack varies with time.

(2) When the sliding direction is selected in the $\langle 1\,0\,0\rangle$ direction, the internal parallel crack under the $\{1\,0\,0\}$ plane develops parallel to the sliding surface and in front of the centre of the slider. The oblique crack propagates towards the front of the slider. The internal normal crack is formed between the top of the oblique crack and the parallel crack. Also, in the $\langle 1\,1\,0\rangle$ sliding direction, the oblique crack initiates from the top of the normal crack and the parallel crack develops from the top of the oblique crack.

(3) The wear volume caused by the surface brittle fracture, like chevron cracks, is a factor of 10 higher than that with surface plastic flow, but the internal cracks are basically independent of the progressing wear.

Acknowledgements

The authors express their appreciation to Professor J. A. Pask (University of California, Berkely) for kind advice and helpful discussions. The authors

also thank K. Suzuki and K. Nishikawa for constructing the apparatus and carrying out the experimental work.

References

1. F. P. BOWDEN and C. A. BROOKES, *Proc. Roy. Soc. Lond.* **A-295** (1966) 244.
2. C. A. BROOKES, J. B. O'NEILL and B. A. REDFERN, *ibid.* **A-322** (1971) 73.
3. A. S. KEH, J. C. M. LI and Y. T. CHOU, *Acta Met.* 7 (1959) 694.
4. B. H. KEAR, A. TAYLOR and P. L. PRATT, *Phil. Mag.* 4 (1959)665.
5. M. S. STUCKE and A. S. WRONSKI, *J. Mater. Sci.* 9 (1974) 911.
6. R. J. STOKES, T. L. JOHNSTON and C. H. LI, *Phil. Mag.* 3 (1958) 718.
7. *Idem, ibid.* 4 (1959) 920.
8. *Idem, ibid.* 6 (1960) 9.
9. T. G. LANGDON and J. A. PASK, "High Temperature Oxides-Part 3, MgO, Al_2O_3, BeO Ceramics: Fabrication, Characterization and Properties", edited by Allen M. Alper (Academic Press, 1970).
10. A. H. COTTRELL, *Trans. Amer. Inst. Min. (Metall.) Eng.* **212** (1958) 192.
11. R. P. STEIJN, *Wear* 7 (1964) 48.
12. *Idem, J. Appl. Phys.* **34** (1963) 419.
13. F. P. BOWDEN and A. E. HANWELL, *Proc. Roy. Soc. Lond.* **A-295** (1966) 233.
14. D. H. BUCKLEY, "Friction, Wear, and Lubrication in Vacuum", NASA SP-277 (1977).
15. T. SUGITA and H. YASUNAGA, *Wear* **40** (1976) 121.
16. T. SUGITA, K. SUZUKI and S. KINOSHITA, *ibid.* **45** (1977) 57.
17. K. F. DUFRANE and W. A. GLASSER, NASA CR-72530, Battelle Memorial Institute, Columbus Laboratories (1969).
18. J. O. SMITH and C. K. LIU, *J. Appl. Mech., Trans. ASME* 75 (1953) 157.

Received 30 August and accepted 3 November 1977.